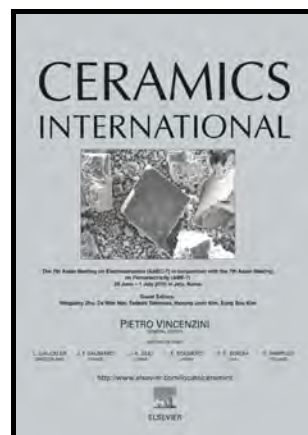


Microwave dielectric properties of novel glass-free low temperature firing  $\text{ACa}_2\text{Mg}_2\text{V}_3\text{O}_{12}$  (A=Li, K) ceramics

Hao Luo, Weishuang Fang, Liang Fang, Wei Li, Chunchun Li, Ying Tang



www.elsevier.com/locate/ceri

PII: S0272-8842(16)30219-X  
DOI: <http://dx.doi.org/10.1016/j.ceramint.2016.03.084>  
Reference: CERI12455

To appear in: *Ceramics International*

Received date: 15 January 2016  
Revised date: 23 February 2016  
Accepted date: 10 March 2016

Cite this article as: Hao Luo, Weishuang Fang, Liang Fang, Wei Li, Chunchun Li and Ying Tang, Microwave dielectric properties of novel glass-free low temperature firing  $\text{ACa}_2\text{Mg}_2\text{V}_3\text{O}_{12}$  (A=Li, K) ceramics, *Ceramics International*, <http://dx.doi.org/10.1016/j.ceramint.2016.03.084>

This is a PDF file of an unedited manuscript that has been accepted for publication. As a service to our customers we are providing this early version of the manuscript. The manuscript will undergo copyediting, typesetting, and review of the resulting galley proof before it is published in its final citable form. Please note that during the production process errors may be discovered which could affect the content, and all legal disclaimers that apply to the journal pertain.

# Microwave dielectric properties of novel glass-free low temperature firing $\text{ACa}_2\text{Mg}_2\text{V}_3\text{O}_{12}$ (A = Li, K) ceramics

Hao Luo<sup>1</sup>, Weishuang Fang<sup>1</sup>, Liang Fang<sup>1,3\*</sup>, Wei Li<sup>3</sup>, Chunchun Li<sup>1,2\*</sup>, Ying Tang<sup>1</sup>

<sup>1</sup>State Key Laboratory Breeding Base of Nonferrous metals and specific Materials Processing, Guangxi universities key laboratory of non-ferrous metal oxide electronic functional materials and devices, College of Material Science and Engineering, Guilin University of Technology, Guilin, 541004, China

<sup>2</sup>College of Information Science and Engineering, Guilin University of Technology, Guilin, 541004, China

<sup>3</sup>College of Materials and Chemical Engineering, Three Gorges University, Yichang 443002, China

## Abstract

Two novel low-firing microwave dielectric ceramics  $\text{ACa}_2\text{Mg}_2\text{V}_3\text{O}_{12}$  (A = Li, K) were prepared using the solid state reaction method. The phase composition, sintering behavior, and microwave dielectric properties were investigated. X-ray diffraction (XRD) analysis showed that both ceramics crystallized into a cubic garnet structure. Both ceramics were well densified at temperatures lower than 960 °C.  $\text{LiCa}_2\text{Mg}_2\text{V}_3\text{O}_{12}$  ceramic sintered at 940 °C with relative density of ~ 96.3% obtained the optimum microwave dielectric properties with  $\epsilon_r \sim 9.8$ ,  $Q \times f \sim 24,900$  GHz (at 11.0 GHz),  $\tau_f \sim +259.2$  ppm/°C. For  $\text{KCa}_2\text{Mg}_2\text{V}_3\text{O}_{12}$ , the ceramic sintered at 900 °C had a relative density of ~ 96.1%, a relative permittivity ( $\epsilon_r$ ) ~ 10, a quality factor ( $Q \times f$ ) ~ 30,330 GHz and a large positive temperature coefficient of resonance frequency  $\tau_f \sim +190.9$  ppm/°C. Both  $\text{ACa}_2\text{Mg}_2\text{V}_3\text{O}_{12}$  (A = Li, K) ceramics were chemically compatible with Ag electrodes. The large positive  $\tau_f$  of  $\text{LiCa}_2\text{Mg}_2\text{V}_3\text{O}_{12}$  ceramic could

\* Corresponding Author: fangliangg1001@aliyun.com; lichunchun2003@126.com

be compensated by forming solid solution with  $\text{NaCa}_2\text{Mg}_2\text{V}_3\text{O}_{12}$ , and improved properties with a near-zero  $\tau_f = +2$  ppm/ $^{\circ}\text{C}$ ,  $\varepsilon_r = 9.9$ ,  $Q \times f = 45,500$  GHz was obtained for  $0.16\text{LiCa}_2\text{Mg}_2\text{V}_3\text{O}_{12}$ - $0.84\text{NaCa}_2\text{Mg}_2\text{V}_3\text{O}_{12}$  ceramic sintered at  $920^{\circ}\text{C}$  for 4 h.

**Keywords:** Microwave dielectric properties; Garnet; Vanadate

## 1. Introduction

In recent years, low-temperature co-fired ceramic (LTCC) has been generating considerable interest due to the requirement of miniaturization and integration [1, 2]. Generally, advanced ceramics for microwave integrated circuits should have a high quality factor ( $Q \times f$ ), a low dielectric constant ( $\epsilon_r$ ), and a near-zero temperature coefficient of resonance frequency ( $\tau_f$ ). Furthermore, for LTCC technology, ceramics should be sintered at temperatures lower than 960 °C (the melting temperature of the inner electrode, such as Ag). Often low-melting point additives are used to reduce the sintering temperatures which results in deterioration of the microwave dielectric properties of the ceramic materials [3, 4].

More recently, some vanadate compounds with garnet structure have been reported to be potential microwave dielectric ceramics for LTCC applications because of their intrinsically low sintering temperatures and promising microwave dielectric properties. For example,  $\text{LiCa}_3\text{MgV}_3\text{O}_{12}$  ceramic sintered at 900 °C has a relative permittivity ( $\epsilon_r$ )  $\sim 10.5$ , a quality factor ( $Q \times f$ )  $\sim 74,700$  GHz and a temperature coefficient of resonant frequency ( $\tau_f$ )  $\sim -61$  ppm/°C [5].  $\text{NaCa}_2\text{Mg}_2\text{V}_3\text{O}_{12}$  ceramic has a  $\epsilon_r = 10$ ,  $Q \times f = 50,600$  GHz and  $\tau_f = -47$  ppm/°C when sintered at 915 °C [6]. By comparison, it is found that the large negative  $\tau_f$  value is a common feature for vanadate garnets (as shown in Table 1). This would impede their practical applications to a large extent. Generally, two approaches have been proposed to adjust the  $\tau_f$  value. The first method is formation of a composite between two compounds with opposite signs of  $\tau_f$  value. In our previous work [6], near-zero  $\tau_f$  garnets were achieved by

compensating the large negative  $\tau_f$  with  $\text{CaTiO}_3$  having a positive one ( $\sim +800$  ppm/ $^{\circ}\text{C}$ ). This approach, in spite of the effective adjustment of the  $\tau_f$  values, could cause an abrupt degradation of the quality factor. Forming solid solution is another accepted method for temperature adjustment. This method is desirable because of its ability to maintain the high  $Q \times f$  while successfully tuning the  $\tau_f$ . Thus, it is worthwhile to search for novel microwave dielectrics with positive  $\tau_f$  values in vanadate garnets as temperature compensators.

The synthesis of  $\text{ACa}_2\text{Mg}_2\text{V}_3\text{O}_{12}$  ( $A = \text{Li, K}$ ) was first reported by Neurgaonkar et al [11]. They reported that both compounds with cubic garnet structure could be easily achieved at  $750^{\circ}\text{C}$  for 24 h. Li *et al.* [12] studied the fluorescence and luminescent properties of  $\text{KCa}_2\text{Mg}_2\text{V}_3\text{O}_{12}$  although so far, their microwave dielectric properties have not been reported yet. In this work,  $\text{ACa}_2\text{Mg}_2\text{V}_3\text{O}_{12}$  ( $A = \text{Li, K}$ ) ceramics were prepared by the conventional solid state reaction method, and its crystal structure, sintering behavior and microwave dielectric properties were studied.

## 2. Experimental Procedure

$\text{ACa}_2\text{Mg}_2\text{V}_3\text{O}_{12}$  ( $A = \text{Li, K}$ ) ceramics were prepared by the conventional solid-state route from high-purity (99%) powders of  $\text{Li}_2\text{CO}_3$ ,  $\text{K}_2\text{CO}_3$ ,  $\text{CaCO}_3$ ,  $\text{MgO}$ , and  $\text{NH}_3\text{VO}_3$  (Guo-Yao Co.Ltd., Shanghai, China). As  $\text{MgO}$  is hygroscopic, it was calcined at  $800^{\circ}\text{C}$  for 2h to remove moisture retains. Powders were milled with zirconia balls for 6h using a planetary mill (Nanjing Machine Factory, Nanjing, China) operating at a running speed of 150 rpm. The mixtures were dried, and calcined at  $700^{\circ}\text{C}$  for 4h, followed by re-milling for 4h. Subsequently, the obtained powder was

mixed with polyvinyl alcohol as a binder and then crushed into a fine powder through a sieve with 200 mesh. The obtained powder was pressed into pellets with 12 mm diameter and 7 mm height by uniaxial pressing under a pressure of 200 MPa. The pellets were heated at 550 °C for 4h to remove the PVA and then sintered at 890-950 °C for 4h. To research the chemical compatibility of  $\text{ACa}_2\text{Mg}_2\text{V}_3\text{O}_{12}$  ( $\text{A} = \text{Li}, \text{K}$ ) with Ag powders, 20 wt% Ag was mixed with the compounds, co-fired at 940 °C and 900 °C for 4h, respectively.

The crystal structure and phase composition of the specimens were analyzed with X-ray diffraction (XRD; Model X'Pert PRO, PANalytical, Almelo, the Netherlands). The bulk densities of the sintered ceramics were measured using Archimedes' method. The surface microstructures of the samples were examined by scanning electron microscopy (SEM; JSM6380-LV, JEOL, Tokyo, Japan). The microwave dielectric properties were measured using a network analyzer (N5230A, Agilent Co., Palo Alto, California) and a temperature chamber (Delta 9039; Delta Design, San Diego, California). The temperature coefficient of the resonant frequency  $\tau_f$  values were calculated with the formula as follows:

$$\tau_f = \frac{f_{85} - f_{25}}{60 \times f_{25}} \quad (1)$$

where,  $f_{85}$  and  $f_{25}$  are the resonant frequencies at the measuring temperatures 85 and 25 °C, respectively.

### 3. Results and Discussion

**Fig.1** shows the XRD patterns of  $\text{ACa}_2\text{Mg}_2\text{V}_3\text{O}_{12}$  ( $\text{A} = \text{Li}, \text{K}$ ) recorded from the calcined powders at 700 °C. All the detected peaks could be indexed based on the

JCPDS file number 00-24-1044 for  $\text{KCa}_2\text{Mg}_2\text{V}_3\text{O}_{12}$ , and no additional peaks were observed. It is notable that the peaks for  $\text{LiCa}_2\text{Mg}_2\text{V}_3\text{O}_{12}$  shifted to higher angle compared with the K-based compound. Both compounds crystallized into a cubic garnet structure with lattice parameter of  $a = 12.3865 \text{ \AA}$  and  $a = 12.5000 \text{ \AA}$  for  $\text{LiCa}_2\text{Mg}_2\text{V}_3\text{O}_{12}$  and  $\text{KCa}_2\text{Mg}_2\text{V}_3\text{O}_{12}$ , respectively. The difference in lattice parameter and the peak shift can be explained by the smaller effective ionic radius of  $\text{Li}^+$  ( $0.078 \text{ \AA}$ ) than that of  $\text{K}^+$  ( $0.151 \text{ \AA}$ ) [13].

SEM micrographs of  $\text{LiCa}_2\text{Mg}_2\text{V}_3\text{O}_{12}$  ceramics sintered at different temperatures ( $920\text{--}950^\circ\text{C}$ ) are shown in **Fig.2**. As shown in **Fig.2** (a), a porous microstructure with an average grain size of  $\sim 2\text{--}3 \mu\text{m}$  was observed. As the sintering temperature increased, the amount of porosity decreased along with a slight increase in the grain size. The sample sintered at  $940^\circ\text{C}$  exhibited a dense microstructure with homogeneously distributed grains and an average grain size of  $\sim 3\text{--}4 \mu\text{m}$ . As illustrated in **Fig.2** (d), some large grains ( $9\text{--}10 \mu\text{m}$ ) appeared in the sample sintered at  $950^\circ\text{C}$ .  $\text{KCa}_2\text{Mg}_2\text{V}_3\text{O}_{12}$  ceramic could be densified at relatively lower temperature ranges ( $880\text{--}910^\circ\text{C}$ ). **Fig.3** shows the SEM images of the surfaces of the sintered  $\text{KCa}_2\text{Mg}_2\text{V}_3\text{O}_{12}$  samples. Similarly, with increasing sintering temperature, the amount of porosity decreased while the grain size increased. A dense microstructure with an average grain size of  $\sim 3\text{--}4 \mu\text{m}$  was observed in the sample sintered at  $900^\circ\text{C}$ .

XRD pattern, backscattered electron image (BSE) and energy dispersive spectrometer (EDS) analysis of the co-fired  $\text{LiCa}_2\text{Mg}_2\text{V}_3\text{O}_{12}$  with 20 wt % Ag sintered at  $940^\circ\text{C}$  for 4 h are shown in **Fig.4**. From the XRD patterns, only the peaks of

$\text{LiCa}_2\text{Mg}_2\text{V}_3\text{O}_{12}$  and Ag (JCPDS No. 004-0783) could be observed and no secondary phase was detected. Two different kinds of grains with different elemental contrast were distinguished and were marked as spots 1 and 2 in the BSE image. EDS analysis revealed that the bright grains (spot 1) were Ag while the slight dark grains (spot 2) were rich in Ca, Mg, and V elements. These results indicate that  $\text{LiCa}_2\text{Mg}_2\text{V}_3\text{O}_{12}$  did not react with Ag when sintered at 940 °C for 4 h. Similar results were observed in  $\text{KCa}_2\text{Mg}_2\text{V}_3\text{O}_{12}$  and the respective XRD pattern, BSE image, and EDS analysis of the co-fired  $\text{KCa}_2\text{Mg}_2\text{V}_3\text{O}_{12}$  with 20 wt % Ag sintered at 900 °C for 4 h are shown in **Fig.5**.

The relative densities of the sintered ceramics are shown in **Fig.6** as a function of sintering temperature. As the sintering temperature increased to 940 °C, the relative density of  $\text{LiCa}_2\text{Mg}_2\text{V}_3\text{O}_{12}$  increased to a maximum value of  $\sim 3.25 \text{ g/cm}^3$  (96.3 % of theoretical density  $3.37 \text{ g/cm}^3$ ), and then decreased slightly due to the over-sintering. A similar change in density was observed for  $\text{KCa}_2\text{Mg}_2\text{V}_3\text{O}_{12}$ . A maximum relative density of  $\sim 3.35 \text{ g/cm}^3$  (about 96.1 % of theoretical density  $3.49 \text{ g/cm}^3$ ) was achieved in the sample sintered at 900 °C. These results are in accordance with the SEM analysis.

The variation of microwave dielectric properties ( $\epsilon_r$ ,  $Q \times f$ , and  $\tau_f$  values) of both ceramics are shown in **Fig.6** as a function of sintering temperature. For both compounds, the variation trend of the relative permittivity and quality factor with increasing sintering temperature is similar to that of the bulk density. The largest  $\epsilon_r$  and  $Q \times f$  values were achieved at the sintering temperatures corresponding to the



highest bulk densities. However, no significant change in  $\tau_f$  value was detected as the sintering temperature increased. As shown in **Fig.6**, the  $\tau_f$  values of  $\text{ACa}_2\text{Mg}_2\text{V}_3\text{O}_{12}$  ( $A = \text{Li, K}$ ) ceramic are about  $255 \pm 5$  and  $188 \pm 2$  ppm/ $^{\circ}\text{C}$ , respectively. The best microwave dielectric properties of  $\text{LiCa}_2\text{Mg}_2\text{V}_3\text{O}_{12}$  ceramic were obtained for the sintering temperature of  $940^{\circ}\text{C}$  with a  $\varepsilon_r$  value of  $\sim 9.8$ , a  $Q \times f$  value of  $\sim 24,900$  GHz, and a  $\tau_f \sim +259.2$  ppm/ $^{\circ}\text{C}$ . For  $\text{KCa}_2\text{Mg}_2\text{V}_3\text{O}_{12}$  ceramic, the optimum microwave properties were obtained at  $900^{\circ}\text{C}$  with a  $\varepsilon_r \sim 10$ , a  $Q \times f$  value of  $\sim 30,300$  GHz, and a  $\tau_f \sim +190.9$  ppm/ $^{\circ}\text{C}$ .

The theoretical relative permittivity can be calculated by the Clausius-Mossotti equation [14, 15].

$$\varepsilon_r = \frac{1 + 2b\alpha_D^T/V_m}{1 - b\alpha_D^T/V_m} \quad (2)$$

where,  $b = 4\pi/3$ ,  $\alpha_D^T$  is the sum of ionic polarizabilities of individual ions and  $V_m$  is the molar volume. The theoretical relative permittivity of  $\text{ACa}_2\text{Mg}_2\text{V}_3\text{O}_{12}$  ( $A = \text{Li, K}$ ) ceramic is 10.4 and 11.9, respectively. This could partly explain the lower  $\varepsilon_r$  of  $\text{LiCa}_2\text{Mg}_2\text{V}_3\text{O}_{12}$  than that of  $\text{KCa}_2\text{Mg}_2\text{V}_3\text{O}_{12}$ .

It is well known that the quality factor ( $Q \times f$ ) is affected by the intrinsic factors like lattice vibration and ionic polarization, and the extrinsic factors, such as grain boundaries, impurities, defects, order-disorder, etc. [16]. In the present system, the effects from secondary phase and impurities could be eliminated based on the XRD and SEM results that confirmed the formation of single phase ceramics with high relative density ( $>95\%$ ).

The  $Q \times f$  strongly depends on the packing fraction [17] which can be calculated

by Eq (3).

$$\text{packing fraction (\%)} = \frac{\text{volume of packed ions}}{\text{volume of primitive unit cell}} \quad (3)$$

The packing fraction of  $\text{LiCa}_2\text{Mg}_2\text{V}_3\text{O}_{12}$  is 68.5%, much larger than that of  $\text{KCa}_2\text{Mg}_2\text{V}_3\text{O}_{12}$  (71.2%). Thus, the  $Q \times f$  of  $\text{LiCa}_2\text{Mg}_2\text{V}_3\text{O}_{12}$  is lower than that of  $\text{KCa}_2\text{Mg}_2\text{V}_3\text{O}_{12}$  might be partly due to the smaller packing fraction.

It is worth noting that the  $\tau_f$  of  $\text{ACa}_2\text{Mg}_2\text{V}_3\text{O}_{12}$  ( $A = \text{Li, K}$ ) ceramic are largely positive. It may be possible to design solid solution between  $\text{ACa}_2\text{Mg}_2\text{V}_3\text{O}_{12}$  and other cubic garnet ceramics with negative  $\tau_f$  values to obtain novel temperature stable microwave dielectrics. More recently, a low-firing garnet ceramic  $\text{NaCa}_2\text{Mg}_2\text{V}_3\text{O}_{12}$  with a negative  $\tau_f \sim -47$  ppm/ $^{\circ}\text{C}$ , a  $\varepsilon_r \sim 10$ , and a  $Q \times f \sim 50,600$  GHz was reported [6]. In this paper, the  $\tau_f$  of  $\text{LiCa}_2\text{Mg}_2\text{V}_3\text{O}_{12}$  ceramic was tuned by forming solid solution with  $\text{NaCa}_2\text{Mg}_2\text{V}_3\text{O}_{12}$ . The microwave dielectric properties of  $(\text{Li}_{1-x}\text{Na}_x)\text{Ca}_2\text{Mg}_2\text{V}_3\text{O}_{12}$  ( $0 \leq x \leq 0.84$ ) ceramic sintered at 920  $^{\circ}\text{C}$  for 4h were shown in Table 2. All the sintered ceramics exhibited high  $Q \times f$  values. The  $\tau_f$  value decreased from +259.2 to +2 ppm/ $^{\circ}\text{C}$  with increasing  $x$  values from 0 to 0.84. The  $(\text{Li}_{0.16}\text{Na}_{0.84})\text{Ca}_2\text{Mg}_2\text{V}_3\text{O}_{12}$  ceramic sintered at 920  $^{\circ}\text{C}$  for 4h showed improved properties with  $\varepsilon_r \sim 9.9$ ,  $Q \times f \sim 45,500$  GHz,  $\tau_f \sim +2$  ppm/ $^{\circ}\text{C}$ .

#### 4. Conclusions

In summary,  $\text{ACa}_2\text{Mg}_2\text{V}_3\text{O}_{12}$  ( $A = \text{Li, K}$ ) ceramics were prepared through a solid-state reaction method. Both ceramics could be well densified at temperatures lower than 960  $^{\circ}\text{C}$ .  $\text{LiCa}_2\text{Mg}_2\text{V}_3\text{O}_{12}$  ceramics exhibited good microwave dielectric properties with a  $\varepsilon_r \sim 9.8$ , a  $Q \times f$  value of  $\sim 24,900$  GHz, and a  $\tau_f \sim +259.2$  ppm/ $^{\circ}\text{C}$ .

For  $\text{KCa}_2\text{Mg}_2\text{V}_3\text{O}_{12}$  ceramic, the optimum microwave dielectric properties were:  $\varepsilon_r \sim 10$ ,  $Q \times f \sim 30,300$  GHz, and  $\tau_f \sim +190.9$  ppm/°C. The large positive  $\tau_f$  of  $\text{LiCa}_2\text{Mg}_2\text{V}_3\text{O}_{12}$  ceramic could be tuned by forming solid-solution with  $\text{NaCa}_2\text{Mg}_2\text{V}_3\text{O}_{12}$ , and the  $(\text{Li}_{0.16}\text{Na}_{0.84})\text{Ca}_2\text{Mg}_2\text{V}_3\text{O}_{12}$  ceramic sintered at 920 °C for 4 h showed improved properties with  $\varepsilon_r \sim 9.9$ ,  $Q \times f \sim 45,500$  GHz,  $\tau_f \sim +2$  ppm/°C. Additionally, XRD, EDS analysis revealed that both ceramics were chemically compatible with silver electrodes at their respective sintering temperatures.

### Acknowledgments

This work was supported by Natural Science Foundation of China (Nos. 21261007, 21561008, and 51502047), the Natural Science Foundation of Guangxi Zhuang Autonomous Region (Nos. 2015GXNSFBA139234, and 2015GXNSFFA139003), Project of Department of Science and Technology of Guangxi (No. 114122005-28), and Projects of Education Department of Guangxi Zhuang Autonomous Region (Nos. YB2014160, KY2015YB341, and KY2015YB122).

## References

- [1] D. Zhou, H. Wang, X Yao, L. X. Pang, Sintering Behavior, Phase Evolution, and Microwave Dielectric Properties of  $\text{Bi}(\text{Sb}_{1-x}\text{Ta}_x)\text{O}_4$  Ceramics, *J. Am. Ceram. Soc.* 91 (2008) 2228-2231.
- [2] M. M. Krzmanc, M. Logar, B. Budic, D. Suvorov, Dielectric and Microstructural Study of the  $\text{SrWO}_4$ ,  $\text{BaWO}_4$ , and  $\text{CaWO}_4$  Scheelite Ceramics, *J. Am. Ceram. Soc.* 94 (2011) 2464-2472.
- [3] R. Umemura, H. Ogawa, A. Kan, Low temperature sintering and microwave dielectric properties of  $(\text{Mg}_{3-x}\text{Zn}_x)(\text{VO}_4)_2$  ceramics, *J. Eur. Ceram. Soc.* 26 (2006) 2063-2068.
- [4] S. X. Dai, R.-F. Huang, D. L. Wilcox, Use of Titanates to Achieve a Temperature-Stable Low-Temperature Cofired Ceramic Dielectric for Wireless Applications, *J. Am. Ceram. Soc.* 85 (2002) 828-832.
- [5] L. Fang, C. X. Su, H. F. Zhou, H. Zhang, Novel Low-Firing Microwave Dielectric Ceramic  $\text{LiCa}_3\text{MgV}_3\text{O}_{12}$  with Low Dielectric Loss, *J. Am. Ceram. Soc.* 96 [3] (2013) 688-690.
- [6] L. Fang, F. Xiang, C. X. Su, H. Zhang, A novel low firing microwave dielectric ceramic  $\text{NaCa}_2\text{Mg}_2\text{V}_3\text{O}_{12}$ , *Ceram. Int.* 39 [8] (2013) 9779-9783.
- [7] H. C. Xiang, L. Fang, X. W. Jiang, C. C. Lei, Low-firing and microwave dielectric properties of  $\text{Na}_2\text{YMg}_2\text{V}_3\text{O}_{12}$  ceramic, *Ceram. Int.* 42 [2] (2016) 3701-3705.

- [8] X. W. Jiang, L. Fang, H. C. Xiang, H. H. Guo, J. Lie, C. C. Lei, A novel low-firing microwave dielectric ceramic  $\text{NaMg}_4\text{V}_3\text{O}_{12}$  and its chemical compatibility with silver electrode, *Ceram. Int.* 41 (2015) 13878-13882.
- [9] H. F. Zhou, F. He, X. L. Chen, J. Chen, L. Fang, Series of thermally stable  $\text{Li}_{1+2x}\text{Mg}_{4-x}\text{V}_3\text{O}_{12}$  ceramics: low temperature sintering characteristic, crystal structure and microwave dielectric properties, *J Mater Sci: Mater Electron* 25 (2014) 1480-1484.
- [10] C. X. Su, L. Fang, Z. H. Wei, X. J. Kuang, H. Zhang,  $\text{LiCa}_3\text{ZnV}_3\text{O}_{12}$ : A novel low-firing, high Q microwave dielectric ceramic, *Ceram. Int.* 40 (2014) 5015-5018.
- [11] R. R. Neurgaonkar, F. A. Hummel, Substitutions in vanadate garnets, *Mat. Res. Bull.* 10 (1975) 51-56.
- [12] J. F. Li, K. H. Qiu, J. F. Li, W. Li, Q. Yang, J. H. Li, A novel broadband emission phosphor  $\text{Ca}_2\text{KMg}_2\text{V}_3\text{O}_{12}$  for white light emitting diodes, *Mate. Res. Bull.* 45 (2010) 598-602.
- [13] R. D. Shannon, Revised effective ionic radii and systematic studies of interatomic distances in halides and chalcogenides, *Acta Crystallogr Sect. A* 32 (1976) 751-767.
- [14] S. H. Yoon, D. W. Kim, S. Y. Cho, H. K. Sun, Investigation of the relations between structure and microwave dielectric properties of divalent metal tungstate compounds, *J. Eur. Ceram. Soc.* 26 (2006) 2051-2054.
- [15] R. D. Shannon, Dielectric polarizabilities of ions in oxides and fluorides, *J. Appl. Phys.* 73 (1993) 348-366.

- [16] N. I. Santha and M. T. Sebastian, Microwave dielectric properties of  $A_6B_5O_{18}$ -type perovskite, *J. Am. Ceram. Soc.* (2007) 90: 496-501.
- [17] E. S. Kim, B. S. Chun, R. Freer, R. J. Cernik, Effects of packing fraction and bond valence on microwave dielectric properties of  $A^{2+}B^{6+}O_4$  ( $A^{2+}$ : Ca, Pb, Ba;  $B^{6+}$ : Mo, W) ceramics, *J. Eur. Ceram. Soc.* 30 (2010) 1731-1736.

Table 1 Microwave Dielectric Properties of Some vanadate garnets

Composition	S. T. (°C)	$\epsilon_r$	$Q \times f$ (GHz)	$\tau_f$ (ppm/°C)	Reference
LiCa <sub>3</sub> MgV <sub>3</sub> O <sub>12</sub>	900	10.5	74700	-61	[5]
Na <sub>2</sub> YMg <sub>2</sub> V <sub>3</sub> O <sub>12</sub>	850	12.3	23180	-4.1	[7]
NaMg <sub>4</sub> V <sub>3</sub> O <sub>12</sub>	690	12.5	35900	-58.1	[8]
LiMg <sub>4</sub> V <sub>3</sub> O <sub>12</sub>	740	10.7	24000	-11.7	[9]
LiCa <sub>3</sub> ZnV <sub>3</sub> O <sub>12</sub>	900	11.5	81100	-72	[10]

Table 2 Bulk density and microwave dielectric properties of (Li<sub>1-x</sub>Na<sub>x</sub>)Ca<sub>2</sub>Mg<sub>2</sub>V<sub>3</sub>O<sub>12</sub> ceramics sintered at 920 °C for 4 h

$x$ value	$\epsilon_r$	$Q \times f$ (GHz)	$\tau_f$ (ppm/°C)
0	9.8	24,900	259.2
0.3	9.8	32,300	165
0.5	9.9	36,750	105
0.7	9.8	40,120	57
0.84	9.9	45,500	2

**Figure Captions:**

**Fig.1** XRD patterns of  $\text{ACa}_2\text{Mg}_2\text{V}_3\text{O}_{12}$  ( $A = \text{Li, K}$ ) powders calcined at  $700^\circ\text{C}/4\text{h}$ .

**Fig.2** SEM micrographs of  $\text{LiCa}_2\text{Mg}_2\text{V}_3\text{O}_{12}$  ceramics sintered at different temperatures: (a)  $920^\circ\text{C}$ ; (b)  $930^\circ\text{C}$ ; (c)  $940^\circ\text{C}$ ; (d)  $950^\circ\text{C}$ .

**Fig.3** SEM micrographs of  $\text{KCa}_2\text{Mg}_2\text{V}_3\text{O}_{12}$  ceramics sintered at different temperatures: (a)  $880^\circ\text{C}$ ; (b)  $890^\circ\text{C}$ ; (c)  $900^\circ\text{C}$ ; (d)  $910^\circ\text{C}$ .

**Fig.4 (a)** XRD patterns of the  $\text{LiCa}_2\text{Mg}_2\text{V}_3\text{O}_{12}$  with 20 wt% silver powder and **(b)** Backscattered electron (BSE) and EDS analysis of the co-fired ceramics.

**Fig.5 (a)** XRD patterns of the  $\text{KCa}_2\text{Mg}_2\text{V}_3\text{O}_{12}$  with 20 wt% silver powder and **(b)** Backscattered electron (BSE) and EDS analysis of the co-fired ceramics.

**Fig.6** The relative densities,  $\epsilon_r$ ,  $Q \times f$  values, and  $\tau_f$  of  $\text{LiCa}_2\text{Mg}_2\text{V}_3\text{O}_{12}$  and  $\text{KCa}_2\text{Mg}_2\text{V}_3\text{O}_{12}$  ceramics sintered at different temperatures.



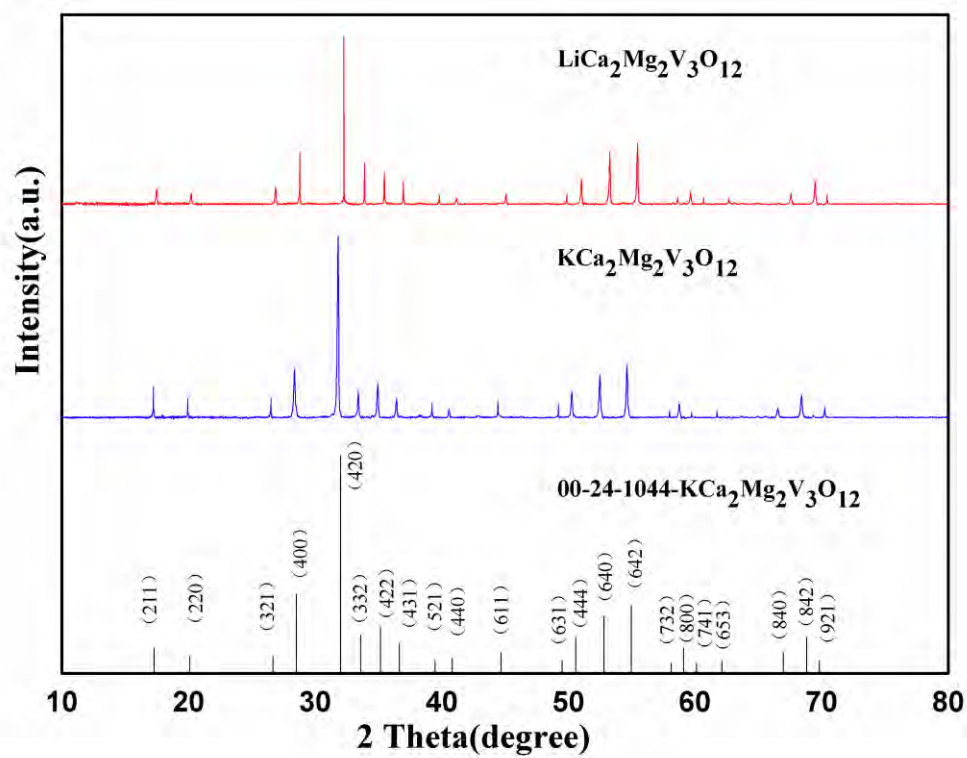


Fig.1

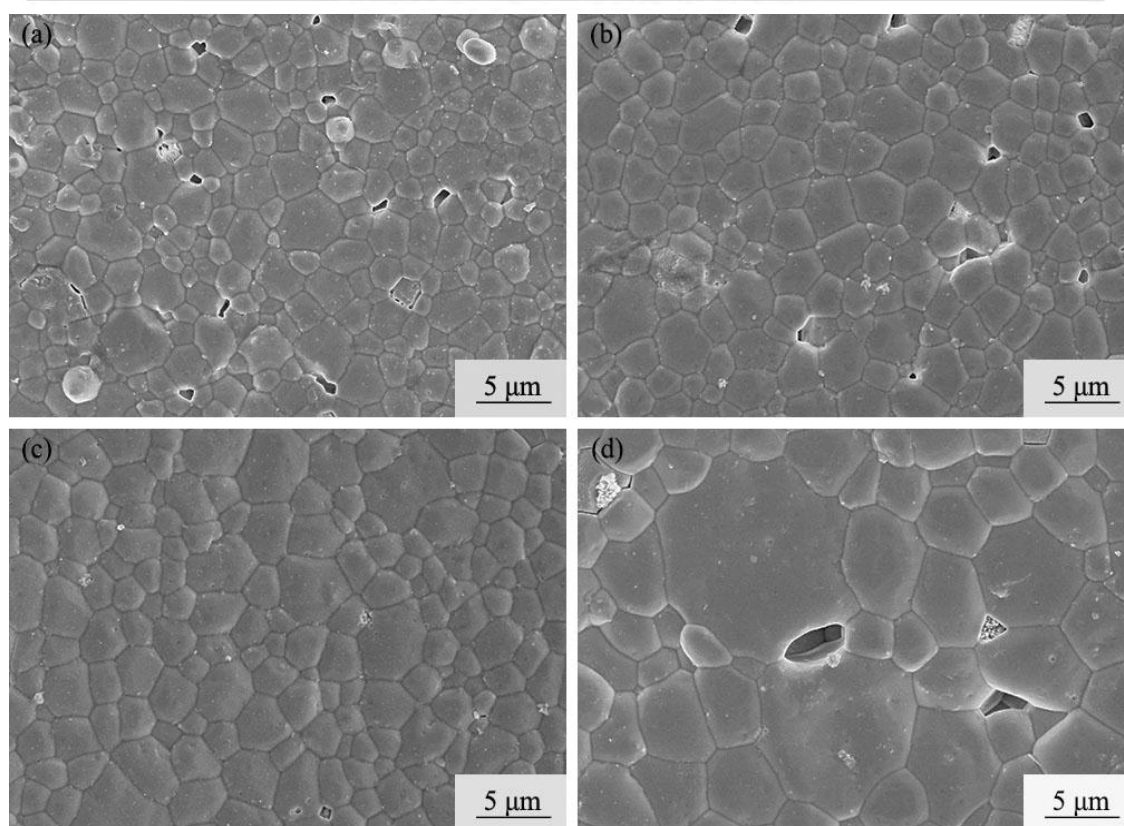


Fig.2

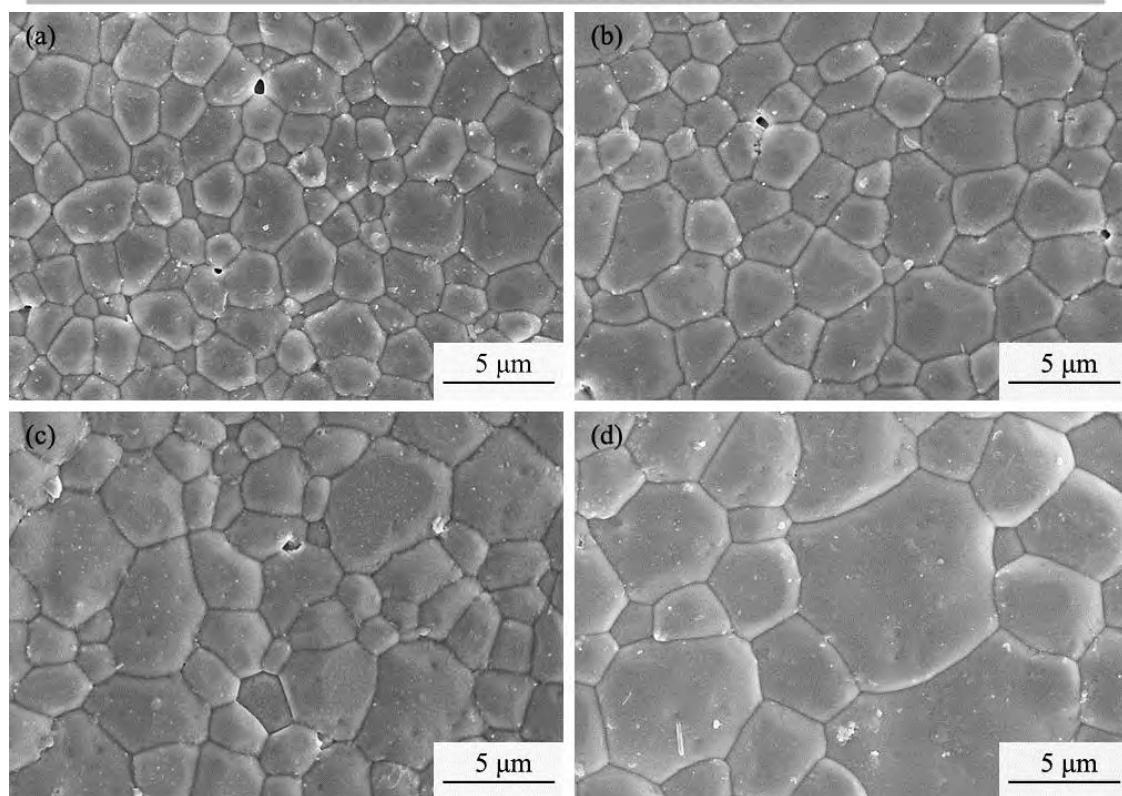


Fig. 3

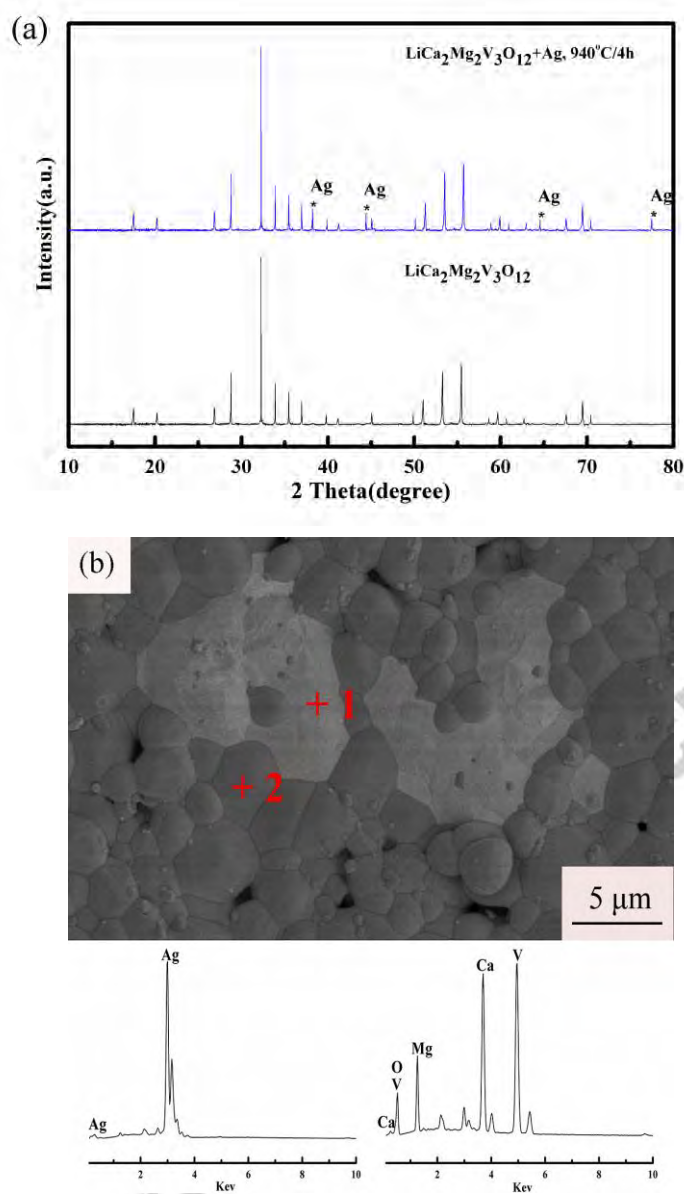


Fig. 4

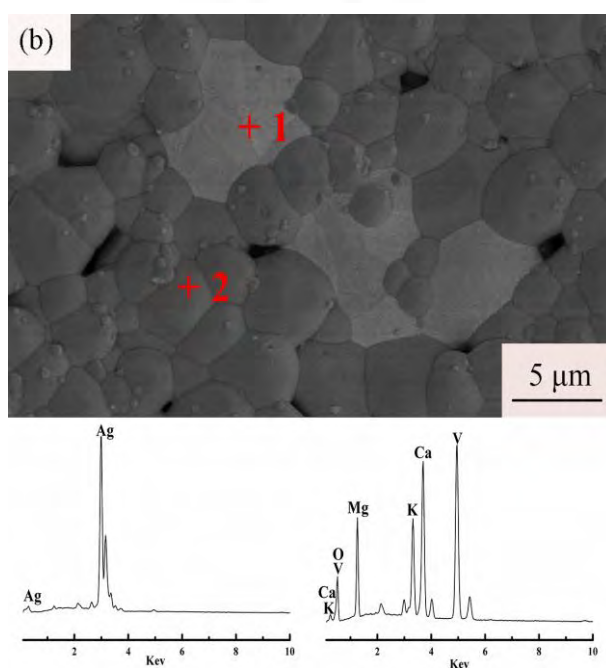
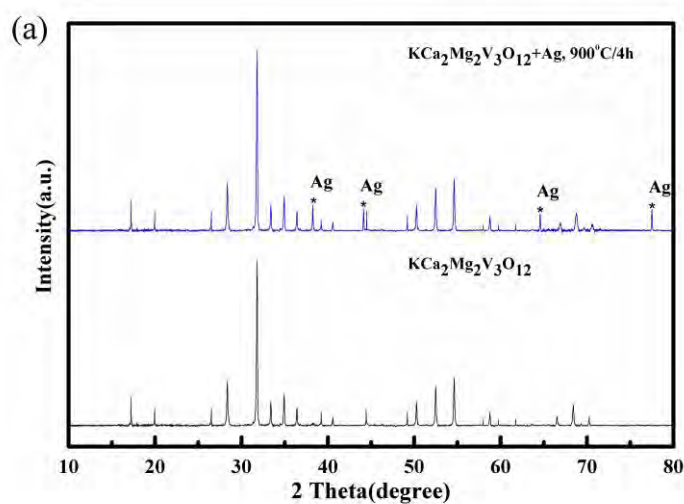


Fig. 5

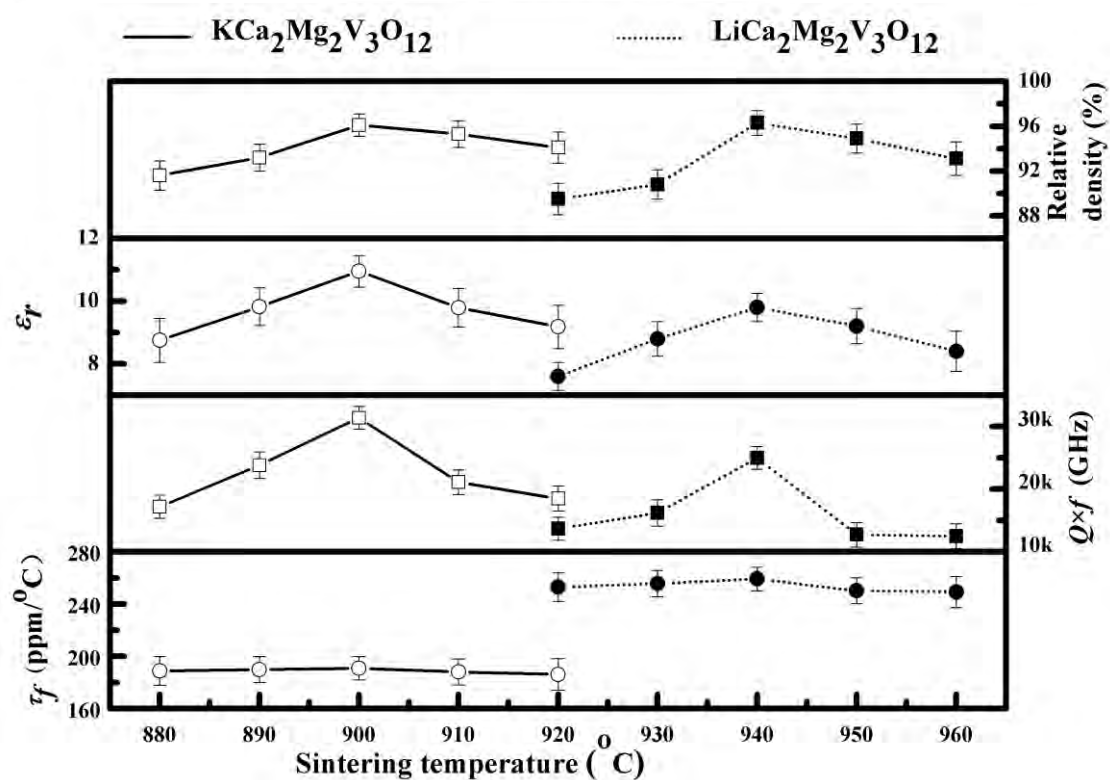


Fig. 6